Rock Mechanics for Natural Resources and Infrastructure
SBMR 2014 – ISRM Specialized Conference 09-13 September, Goiania, Brazil
© CBMR/ABMS and ISRM, 2014

Gas-Shale Fracturing and Fracture Mobilization in Shear: *Quo Vadis*?

Nick Barton
NB&A, Oslo, Norway, nickrbarton@hotmail.com

Eda Quadros
BGTech, São Paulo, Brazil, edafquadros@gmail.com

SUMMARY: The conversion of a highly impermeable medium like shale into numerous gas producing 'pay zones', using geomechanics steered, stress-and-structure oriented hydraulic fracturing, is a remarkable achievement. So remarkable in fact that shear mobilization of natural fractures has also to be invoked to explain both the continued though declining production and the sources of larger 'radius' microseismic activity well beyond the assumed ellipsoidally-shaped tensile-fractured and sand-propped 'central' zones. The microseismic activity is believed to be the remote-sensing sign of shearing *initiation* of a large number of the natural fractures. The assumed shearing, and the resulting gas drainage, cannot occur in the case of gas-shales unless the shale is of high enough modulus to sustain the shear induced dilation, which results in a coupling with enhanced fracture permeability. The pre-peak mobilization of roughness and permeability due to pre-peak dilation, combined with low in situ shear stiffness due to block-size related scale effects, is part of the rock mechanics reality behind critically stressed fractures, which are simplified as linear Mohr Coulomb events in petroleum geomechanics. In reality a more sophisticated and more favourable series of coupled processes are likely to be involved.

KEYWORDS: hydraulic fracturing, fracture shearing, dilation, permeability, coupling

1 INTRODUCTION

Shale gas is one of the unconventional sources of natural gas, which has remained trapped in shale, a sedimentary rock which originates from sedimentary deposits of clay, mud, silt and organic matter. The gas must pass through pore spaces that are 1,000 times smaller than in a conventional sandstone reservoir. The gas production, causing large pressure drop even in the first 250 days, depends on multi-stage hydraulic fracking from wells deviated to give long horizontal sections. The remarkable success, starting in the USA, has justified exploration and production. However the local cost to the environment, and the difficulty with sufficient water supply and disposal of fluids are remaining questions, especially in populated areas. Environmental concerns include gas migration and ground-water contamination due to the processes of well construction. However, communication between the fracked region and near-surface groundwater supplies appears to be impossible, due, usually, to thousands of intervening meters of rock. Some of the evidence for this containment, which of course is fundamental to general acceptance of this technology, will be reviewed in the next few pages.

2 FRACKING HORIZONTAL WELLS

Hydraulic fracturing is a well stimulation technique which has been employed in the oil and gas industry since 1947. There are two primary methods to produce shale gas: vertical multi-stage hydraulic fracturing,

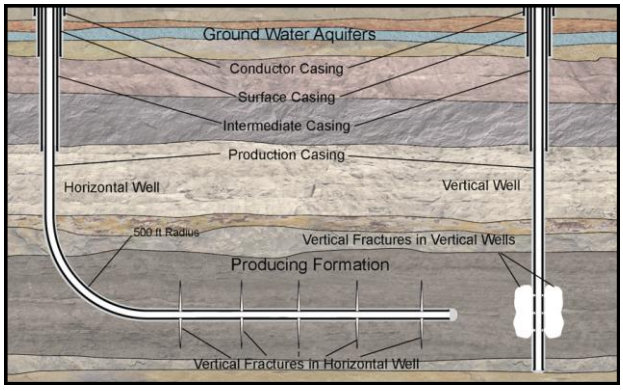

Figure 1. The two options: horizontal and vertical wells. (American Petroleum Institute, 2009).

which was used initially, but is now seldom used, and multi-stage hydraulic fracturing from long horizontal wells. These two options are shown in Figure 1. In the long horizontal-well option, the wellbore is exposed to as much of the shale reservoir as possible, and both the well and the multiple hydraulic fractures will also tend to intersect more natural fractures.

Fracking involves injecting fluid at a very high pressure into the underground rock formations in order to fracture the rock. The low viscosity ('slick' water) fluid pumped down the well is loaded with suitable proppant material, typically sand, which helps to keep the initial ellipsoidally-shaped tensile fractures open and allows the gas to escape from the shale via surrounding natural fractures. The latter are believed to have been shear-stimulated and slightly dilated, thereby greatly increasing the area available for gas release from the matrix, and allowing drainage to the propped regions, and finally to the perforated sections of the wells. The presumed shearing of numerous peripheral natural fractures are the source of microseismic signals. Some rock mechanics aspects of sheared fractures and coupled behaviour will be discussed later.

Horizontal wells are typically drilled vertically to a "kick-off" point where the drill bit is gradually turned from vertical to horizontal. Horizontal drilling that can extend 3 to 5 km vastly increases the wellbore's contact with the gas-bearing formation in relation to vertical drilling, which would be limited to the

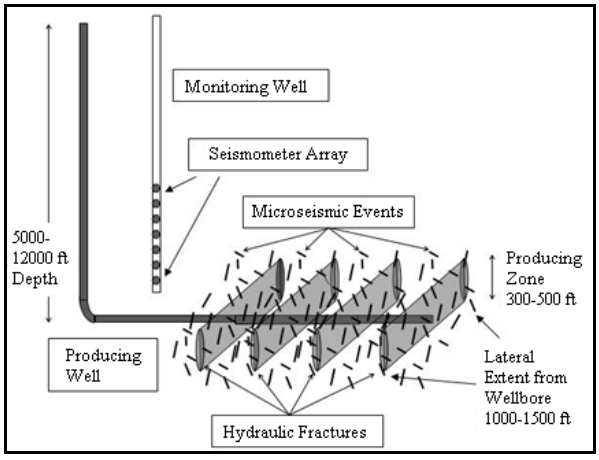

Figure 2. Schematic multiple-stage fracking in a horizontal borehole symbolizing the bed-limited hydraulic fractures produced and the surrounding microseismic events. In this case the producing zone varies from ~100 to 150m. Zoback et al, (2010).

thickness of the formation, which is reportedly 100-200 m in most major U.S. shale plays.

3 MICROSEISMIC DUE TO FRACKING

When multi-stage hydraulic fracturing is performed, numerous microseismic events are recorded in the rock surrounding the hydraulically fractured and sand-propped central system of (mostly) tensile fractures. Figure 2 from Zoback et al. 2010, shows schematically the bed-limited hydraulic fractures produced, and surrounding micro-seismic events which occur in horizontal multi-stage fracking. The induced seismic events are so small that they can only be detected by using highly sensitive seismometers placed in nearby monitoring wells. The seismic monitoring of the rock has given the clue that shearing is also involved. It appears from the extensive microseismic monitoring of fracking operations in all the major shales in the US, as reported in the studies of Warpinski et al. (2011), that seismic magnitudes are always below magnitude 1. Likely slip areas, which may be block-size related when first initiated, and displacements sufficient to be several times larger than the small highly stressed fracture apertures will be discussed later.

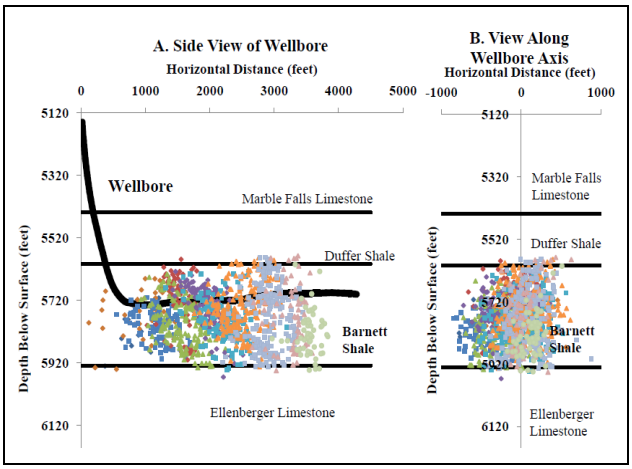

Figure 3 Microseismic resulting from hydraulic fracturing in the brittle Barnett Shale, USA signifies shearing of fractures. Each colour represents recordings due to a distinct fracturing stage. Zoback et al. (2010).

Figure 3 shows typical microseismic activity at depths of nearly 6 km in the most-brittle and highest-modulus Barnett Shale (USA). The 'cloud' of activity occurs both above and below the wells. Each of the dots in A and B represents a microseismic event caused by the effect of the hydraulic fracturing on the surrounding natural fractures, which are presumed to have had a slight but important shearing event initiated.

The principal horizontal rock stresses are the most significant source of constraint on fracture growth. Following the elasticity theory, hydraulic fractures propagate perpendicularly to the direction of least principal stress, and in the direction of maximum principal stress. However in the vertical direction, the fractures will extend until they reach a more ductile rock material. Materials such as softer shales are more difficult to fracture than brittle shale rocks. These ductile layers provide the constraint and can cause the remaining fracture to travel horizontally within the more brittle layer. This also provides desirable contact area.

Figure 4 shows the relationship between depth and orientation of fracture growth in sedimentary formations as recorded and interpreted by Fisher and Warpinski (2012). Each point on the figure represents a separate fracture treatment from more than 10,000 fractures mapped using tiltmeters throughout

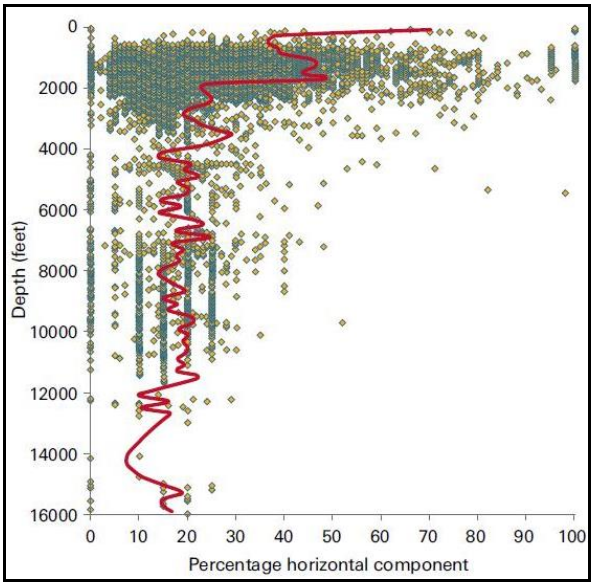

Figure 4 Relationship between depth and orientation of fracture growth in sedimentary formations. Sub-vertical fractures are shown to predominate at depth. Fisher & Warpinsk (2011).

the past decade, in numerous sedimentary formations, including shales in the USA. Figure 5 shows the vertical dimensions of hydraulic fractures in Eagle Ford, Woodford, Barnett, Marcellus and Niobrara shales after Fisher and Warpinski (2011).

The hydraulic-fractures heights are relatively well contained. The directly measured height growth is reportedly often less than conventional hydraulic-fracture propagation models used for prediction, because some of the containment mechanisms (e.g. dissipation in a plastic layer, or perhaps leak-off into a discontinuity) may not be considered in the models. Concerning possible proximity to water supplies, we can conclude from Figure 6 and other equally extensive data sets collected by Fisher and Warpinski (2011), that there is significant physical separation between hydraulic-fracture tops and aquifers, which usually amounts to several thousands of meters of intervening rock.

4 POSSIBLE STYLES OF H-FRACTURES

Figure 7 is a schematic showing the possible hierarchy of complexity of hydraulic fractures

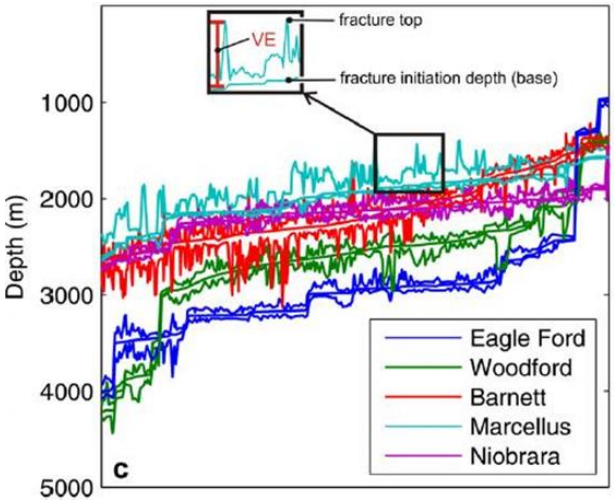

Figure 5 Diagram showing the typical height of the hydraulic fractures as recorded in the principal shale plays in the USA. Fisher and Warpinski (2011).

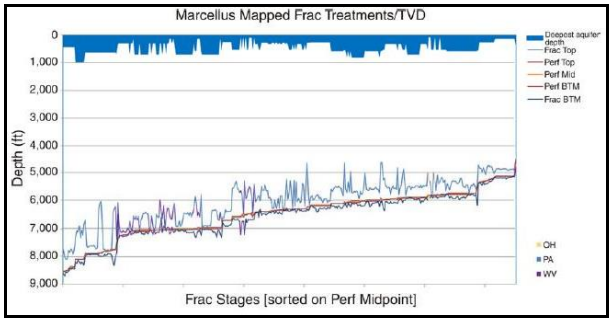

Figure 6 Measured fracture heights sorted by depth and compared to aquifers in Marcellus shale. Fisher and Warpinski (2011).

in practice (Fisher, 2002; Warpinski et al. 2010). The authors point out that instead of the simple planar fracture (upper left), fractures in common geologic environments may show varying degrees of complexity, from the simple complex fracture that is relatively planar (upper right), to the complex fracture network (lower right). These are apparently principal-stress related, as in the illustrations of McLennan and Potocki (2013), based on Shylapoberski, shown in Figure 8.

As a result of this complexity, the hydraulically-driven near-well fractures apparently tend to grow shorter than they would if they were singular planar features. The multiple strands provide additional wall areas that

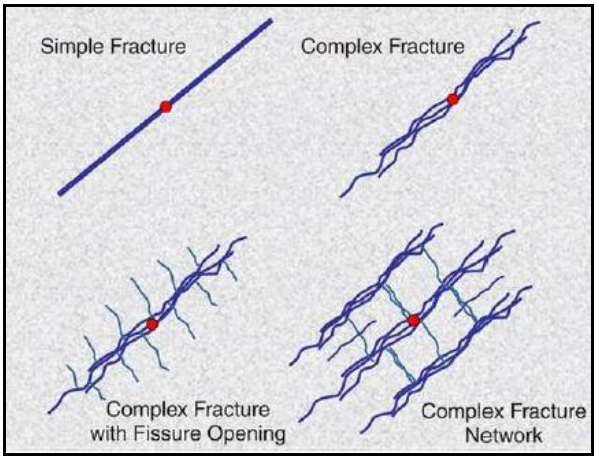

Figure 7 Schematics of assumed levels of complexity of hydraulic fractures, as occasionally observed in mine-backs. Fisher and Warpinski (2011).

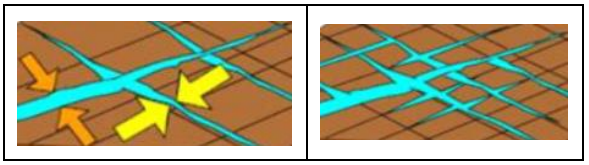

Figure 8 Modified from sketches in McLennon and Potocki (2013) concerning the influences of multi-fracked branches on ISIP, due to the attempt by the two in situ stress components to force fluid back to the perforations.

increase friction and thus raise the necessary fluid pressure, causing wider cracks. The additional walls also provide a large amount of added surface area for leak-off of the injected fluid. As a result, complex fractures are shorter and wider than simple fractures, and both their height growth and length growth are reduced.

Given this complexity in a relatively simple fracturing environment, it is clear that the height-growth mechanisms in a complex sedimentary basin that is also perturbed by structure and natural fractures, will likely be influenced by the layering and heterogeneities of both the local layer properties (like modulus) and the probably related local stress magnitudes.

In minifrac stress measurements performed by Barton (1981), while working with TerraTek, the minimum principal stresses were ‘proportionally’ related with the increasing moduli of the shale, siltstone and sandstone inter-beds. However at greater depth in oil reservoirs, it is the lack of resistance to shear

Figure 9 The relative planarity of fractures in shale seen in sectioned core, from Gale et al. (2011), in a pavement outcrop, from Han (2011) and in a Kimmeridge Bay cliff outcrop of shale source-rock, from Barton (2014).

stresses which may determine the minimum stress contrasts between a cap-rock shale and the sandstone reservoir inter-beds (Barton, 1986). The minimum principal rock stress will be lowest for shale at shallow depth, but highest for (cap-rock) shale at much greater depth.

5 NATURAL FRACTURE MOBILIZATION

Quite planar examples of natural fractures are illustrated in Figure 9. The indirect stimulation of such natural fractures in shear, appears to be the key to sustained production from gas-shale reservoirs. Some incidences of shearing, which could also apply to the hydraulic fractures, are illustrated in Figure 10. It is necessary to increase the surface area of shear-stimulated fracturing, so that gas can leave the matrix

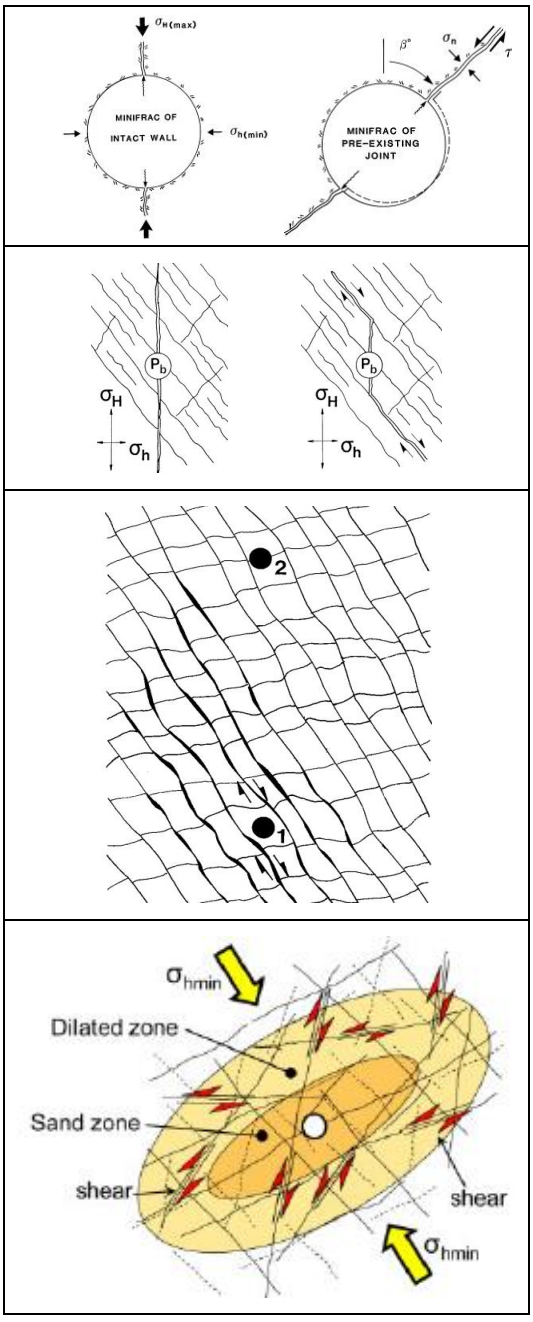

Figure 10 Alternative scenarios involving fracture shearing (minifrac and geothermal energy), from Barton (1981) and Barton (1986). The lowest figure is specific to gas-shale stimulation, and is the Dusseault (2013) indication that shearing of fractures outside the sand-propped zone is the source of microseismic activity and the key to production from 'impermeable' gas-shales.

due to the greatly increased permeability. Nevertheless there appears to be concern in some parts of the industry about the quite rapid decline in pressure, and therefore the quite rapid decline in production. Many tens of MPa can be lost during for instance 250 days of (perhaps)

too rapid production. The ability to shear natural fractures around the peripheries of the 'ellipsoidally' propped region, in order to gain surface area, appears to be the key to maintenance of flow, as stated in King (2010). Detecting the location of natural fractures and optimizing their response to the 'central' hydraulic fracture stimulation volume, seems to be of prime importance. Multiple in-well tools and methods can directly or indirectly help identify *in-situ* fracture characteristics, including their existence, density, orientation, and possibly give an indication of their potential aperture. Natural fracture patterns can also be detected from outcrops. Although outcrop rock may have been subjected to multiple cycles of tectonic movements, and of course surface erosion, the general consensus is that a well-exposed outcrop analogue can provide a generic print of possible in-situ fracture networks, including orientation, pattern, openness, and complexity (Han, 2011). Nevertheless, the potential *non-linearity* of the strength envelope when weaker rocks are strongly loaded (by reduced gas pressures) should not be forgotten when considering extrapolation of the angular relationships of fracturing to higher stress levels. See for instance Barton (2014).

The integration of natural joints or fracture sets in the production of shale gas requires both belief in and confirmation that the clouds of microseismic, detected well outside the frac-simulated and sand-propped region, actually signifies the mobilization of joints or fractures in shear. Away from the high-volume, high-pressure fracking fluid (and sand-propped) entrance into the hydraulically-fractured and naturally-fractured gas-shale, conditions may exist for fracture-shearing stimulation. This may occur where e.g. slick-water is still invading the formation, just beyond the sand-propped region.

An exaggerated view of the shear-dilation mechanism for the case of a rough fracture (where the various phenomena are more easily demonstrated) is shown in Figure 11. The message from this figure is that if shearing stimulation can amount to as much as post-

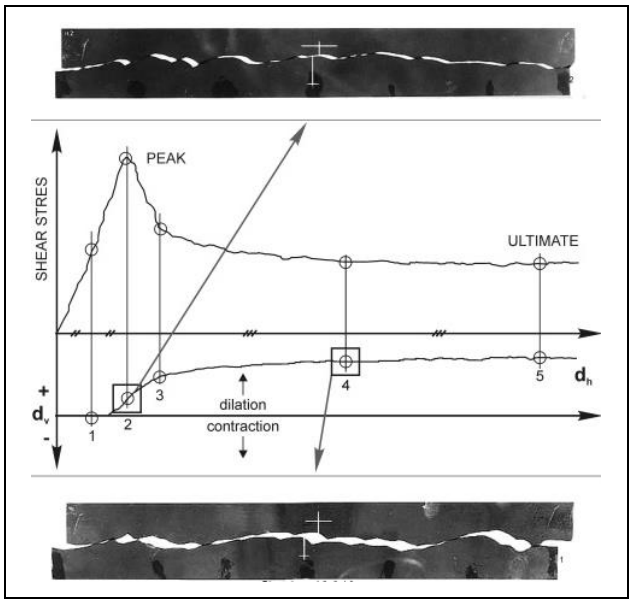

Figure 11 Exact shear-dilation replication from direct shear tests on very rough tension fractures. These were reported by Barton (1973). The roughness profiles were recorded by photogrammetry because of the fragility.

peak, the likelihood of 'shear-propped' fractures being maintained is improved. Note that the contacting and actually over-lapping asperities represent crushed material, and would have resulted in so-called gouge production. Olsson and Barton (2001) have shown how this can be accounted for when converting the larger physical joint aperture (E) into the smaller hydraulic aperture (e). It involves use of JRC_{mob} which is a measure of the amount of mobilization of the joint- or fracture-roughness. An example of the appearance of a sheared non-planar fracture surface in shale, following a coupled shear-flow test, is shown in Figure 12.

In the numerous early coupled shear-flow experiments performed in rock mechanics in the mid-eighties, some one to three orders of magnitude increase in conductivity was registered with only a very few millimeters of shearing, as shown by Makurat et al. (1990). Such increases also led to an understanding of the coupling of shearing and the almost maintained permeability during the ongoing compaction of the Ekofisk chalk reservoir, which now exceeds 10 meters.

The CSFT coupled shear flow test also relied on the combination of sufficient static modulus

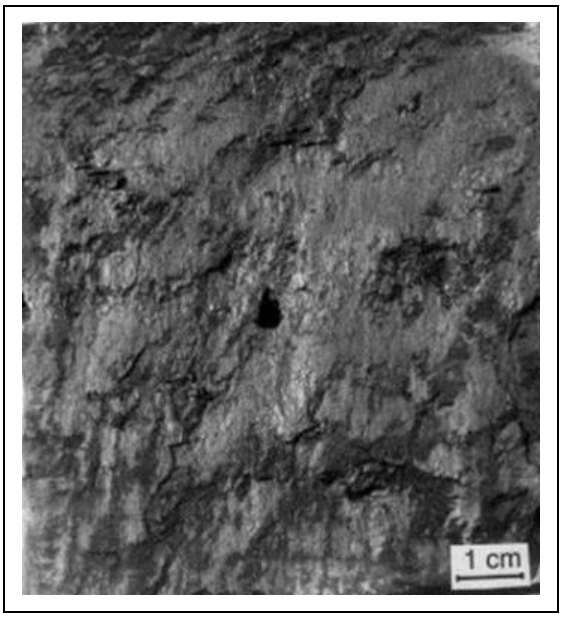

Figure 12 The appearance of a sheared and flow tested natural fracture in Kimmeridge shale. The shale is weak and only 1 MPa normal stress was applied in this test. From Guttierez et al. 2000.

E_{mass} and sufficient in situ scale joint wall compressive strength JCS_n to maintain the effect of the shear-induced dilation. For dilation to occur at least some level of joint or fracture roughness JRC_n is required, despite the typical near-planarity often seen in shales.

Interesting and extensive joint-industry studies were recently reported by Ghassemi and Suarez-Rivera, 2012 from respectively Texas A&M University and TerraTek/Schlumberger. The selected and very small part of the reported studies reproduced in Figure 13 were concerned with the pressure-sensitive conductivity measured during the high-pressure flow tests through artificial saw-cuts or tension fractures in various shales. The latter were displaced 1 mm to (crudely) represent a 'sheared' fracture, based on the assumption that asperities would be crushed. Of course this does not produce the same result as CSFT (coupled shear-flow tests) as reported by Makurat et al., 1990. These more realistic tests were used in Ekofisk reservoir compaction studies, using natural fractures in the chalk. (Barton et al., 1988).

None of the surfaces tested at TerraTek/Sclumberger appear to have directly represented *natural fractures* in the shales,

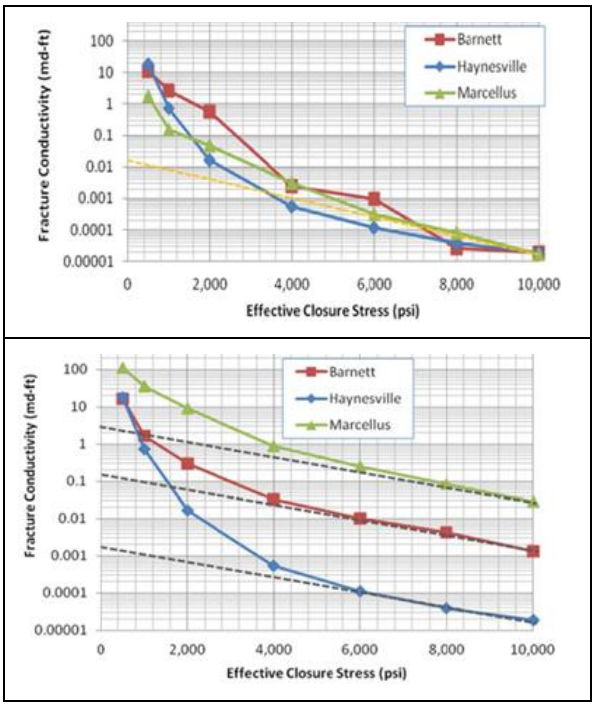

Figure 13 High pressure 'fracture' conductivity tests conducted (top): in saw-cut samples and in 1 mm displaced-before-loading tension fractures. Ghassemi and Suarez-Revera, 2012. The dotted lines show two decades of conductivity reduction over the increment of 69 MPa (10,000 psi) closure stress. Temperature increase reduced conductivity, presumably due to rock strength reduction.

though judging (only) by the appearance of the three examples assembled in Figure 9, perhaps the saw-cuts were quite representative of the typical planarity of fractures in shale, assuming there were no traces of saw-cut 'ridges'. These authors assumed that conductivities poorer than approx. 0.01 md-ft may be too small to support flow at pressures > 2000 psi (≈ 14 MPa). They therefore concluded that unpropped 'secondary and tertiary fractures' should be excluded from models. It is not immediately clear whether the TerraTek/Sclumberger/Texas A & M study tried also to quantify the potential contribution of the possibly aseismically-sheared fractures outside the hydro-fracked and propped region.

6 MODELLING NON-LINEAR BEHAVIOR

Concerning the strong coupling of conductivity and closure pressure seen in Figure 13, it may be useful to see the rock mechanics response of

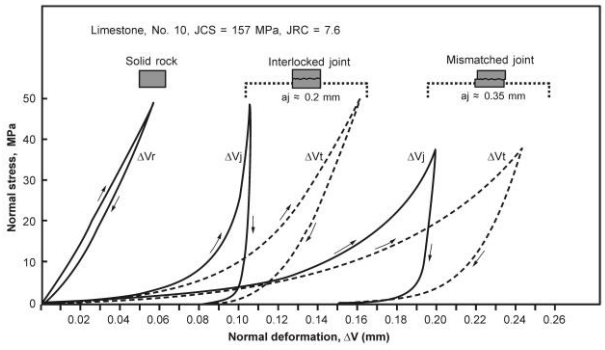

Figure 14 If a previously interlocked joint or fracture is displaced by shearing it has lowered normal stiffness. These stress-closure curves are from Bandis et al., 1983.

normal stiffness to (slight) shearing, like the *artificial* 1mm pre-test displacement. Figure 14 shows the 'softening' closure response of a hard slightly displaced joint surface in limestone with the given properties. Figure 15 by contrast shows the coupled response of an *interlocked* joint to normal stress. Note that aperture E > e.

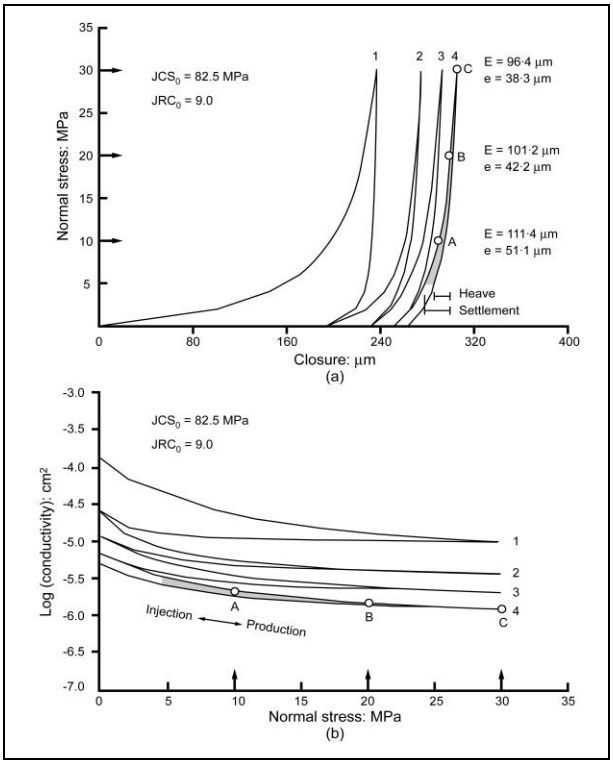

Figure 15 An illustrative set of stress-closure and conductivity-stress curves, based on the 'cycling-to-considate' principle used in Barton-Bandis modelling. Note that the stress range is half of that shown in Figure 13, and also that the modelled small-scale JCS_0 and JRC_0 values are likely to be significantly higher than for most gas-shales, with the possible exception of the Barnett shale. Barton et al. (1985).

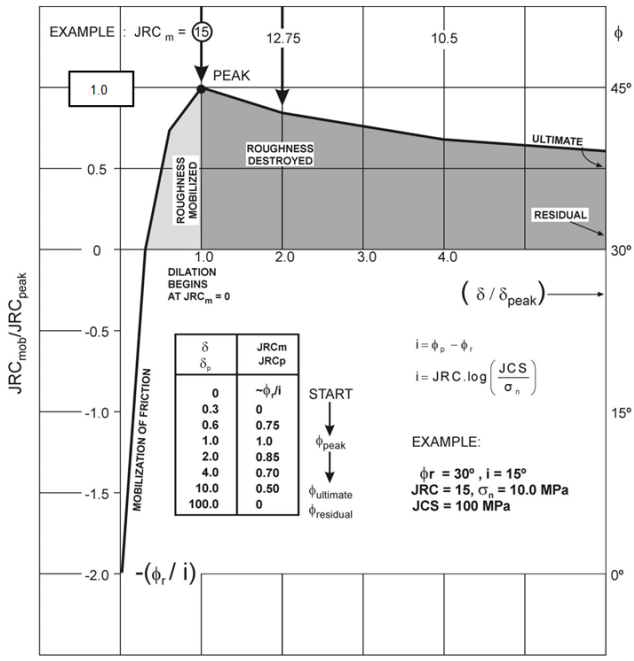

Figure 16 An essential part of coupled process modelling involving joint or fracture shearing is the ability to track shear deformation. This dimensionless method also provides input for modelling dilation. Barton, 1982.

The non-linear behaviour illustrated includes the differentiation of average physical aperture (E) and the theoretical smooth-wall hydraulic aperture (e). The dimensionless quantities (JRC_{mob}/JRC_{peak} and δ/δ_{peak}) represented in Figure 16, have the effect of consolidating all experimental shear test results into one narrow band with the approximate shape shown here. We can therefore use this single device to generate widely different shear stress-displacement and dilation-displacement curves for any desired input data (including variable block size and variable effective normal stress, as shown in Figure 17. The 'look-up' table of values (see inset in Figure 16) is smoothed in the UDEC-BB sub-routine in Cundall's distinct element code. UDEC is well known in the rock mechanics profession, but seems to have been seldom used in petroleum geomechanics. Shear stiffness (Ks) values measured by the first author and collected from the literature (many hundreds of cases), suggest that values may be in the range 2 to 10 MPa/mm when reservoir pore pressures are high, assuming block-sizes (cross-joint spacings) 0.1m < L_n < 1m. However

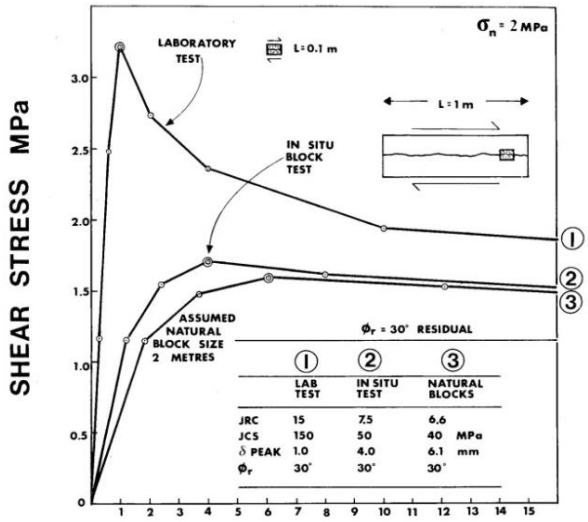

Figure 17 Block-size scaling effects as demomstrated here, are maximised at low normal stress (only 2 MPa in these three examples). Note that peak shear stiffness Ks (= $\tau_{peak}/\delta_{peak}$) is doubly scale-dependent, so *in situ* fractured gas-shale should be easier to stimulate in shear than if testing a laboratory-scale sample. Barton (1982).

as effective stresses rise by tens of MPa during e.g. the first year of production, the resistance to shear will rise and shear stiffness values may be as high as 10 to 50 MPa. This is still lower than the unrealistic values seen in some literature. The potential one to two orders of magnitude increase in conductivity shown in Figure 18 might be more impressive in the case of a deeply buried *hard* gas-shale, because the joint- or fracture- apertures are likely to start (pre-shear) with micron-size apertures, while in the above example, the 'starting' hydraulic aperture has been assumed as a much larger 25μm. On the other hand, weaker gas-shales with lower JCS_0 (joint- or fracture-wall compressive strengths) might dilate only marginally with shear, when gradually more heavily loaded due to production-induced increases in stress.

7 IS SLIP AREA MISINTERPRETED?

The 'clouds' of microseismic events reproduced from Warpinski and colleagues impressive work in earlier figures in this paper, represent very low-energy (low moment) events. The definitions of the moment and magnitude of

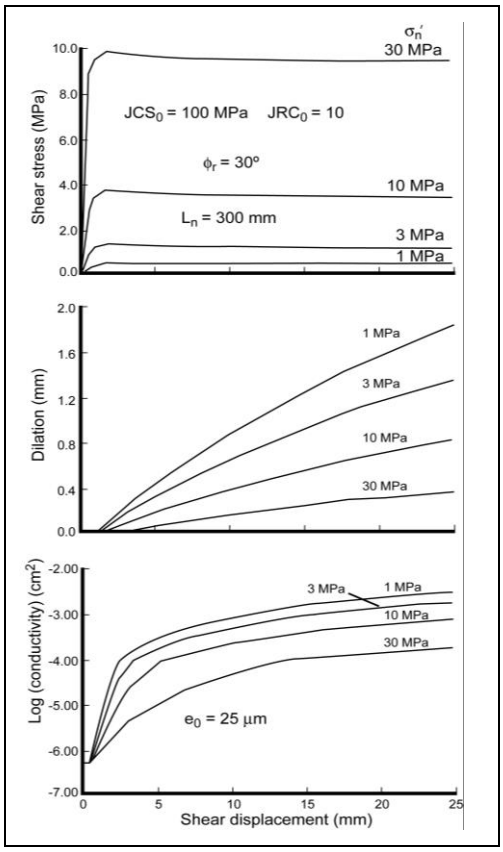

Figure 18 Modelling of shear stress-displacement, dilation-displacement, and (assumed) gouge-free conductivity-displacement, from Barton et al. (1985). Note that the small-scale (nominal 100 mm) values of joint wall strength JCS_0 and joint roughness coefficient JRC_0 are scaled to the assumed L_n = 300 mm *in situ* block size.

an earthquake, which apply to microseismic events as well, are based on the well-known equation:

$$M_0 = \mu dA \qquad (1)$$

where μ is the shear modulus, d is the slip distance and A is the area involved in the seismically recorded event. Perhaps due to a focus on showing the insignificance of the shear displacements, these authors 'composed' examples of slip area (or radius) that seem high, giving (through equation 1) displacements that were very low. For instance the 'central' value in Figure 19: a moment of 1.0^6 ft - lbf, suggests a magnitude of between -1 and -2. These magnitudes can imply a range of (large) fracture radii of e.g. 6m to 11m, slipping only 0.69 to 0.74 μm. If on the other hand the interpreted slip is related to fracture slip in shale with

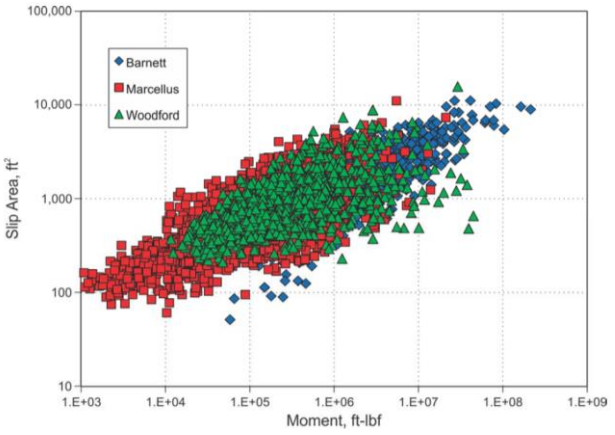

Figure 19 Examples of possible combinations of slip areas and moments, from Warpinski et al., 2012.

much smaller (but more numerous) *block-size related fracture sizes*, then the estimated slip can easily be ten times larger, and amount to, for instance, 10-times the pre-shear micron-size apertures. The assumed shear modulus μ can range from 5 to 25 GPa.

It seems probable, though is an unknown, that *aseismic* slip much larger than '5-10 micron-size', can continue to stimulate the gas drainage, due to the ease of shear when there is only slight dilation. However, and this is truly a 'quo vadis' question: will the shale be strong enough to remain 'naturally shear-propped'?

8 MODULUS AND STRENGTH NEEDS

It is important to note from the review of King, 2010, that only shales with relatively high static deformation moduli will be good candidates for gas production. Non-prospective shales, as shown in Figure 20 in red, apparently have moduli too low e.g. 2-20 GPa to sustain productive propped-fractures and sheared-fractures. Values of 20 to 65 GPa – i.e. very 'rock-like' values, are apparently needed. Concerning the strength related Brinell hardness, Barnett shale has values (≈80) some five times higher than coal (≈15), while Marcellus shale is twice the value of coal.

In view of the fact that the strengths of shales are limited in relation to hard crystalline rocks and to hard carbonaceous rocks, it is appropriate to end this paper with a suggestion

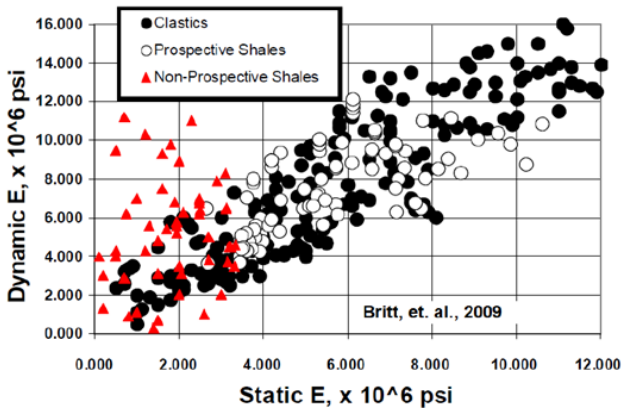

Figure 20 Correlation of Young's modulus between static tests on cores, and dynamic logs. The prospective gas producing shales group with the tight sandstone clastics, while the non-productive shales have a low static modulus and scattered dynamic modulus (King, 2010).

of the strong likelihood that shales will reach the brittle-ductile transition and even *critical state*, as represented in Figure 21, during their production due to the effective stress increase.

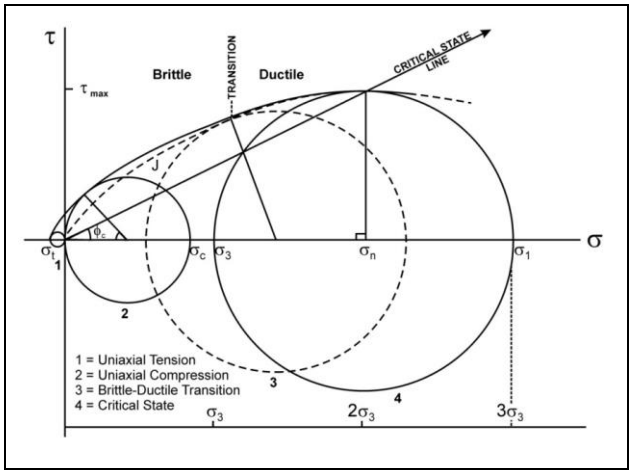

Figure 21 The critical state concept suggested by Barton (1976). This has recently been used by Singh et al. (2011) to derive the equations giving the *correct deviation* from the so frequently used linear Mohr-Coulomb assumption. Just a few triaxial tests at low confining pressure give the complete curved envelope. This is not the case with other criteria. Tests are needed at many different confining pressures when inaccurate linear criteria are used, as so often seen in petroleum geomechanics.

According to the studies of Singh et al. (2011), the majority of rock types have $\sigma_{3\ (critical)} \approx \sigma_c$.

In other words Mohr circles #2 and #4 are touching or nearly touching, as indeed illustrated in Figure 21. There is reason to believe that this non-linearity will be especially relevant in weaker (more clay-bearing) shales, as effective stresses increase during production.

Because some of the other producing gas-shales are significantly weaker than the Barnett shale, it is certain that effective confining stress levels will rise during production to levels exceeding, in some cases, their $\sigma_{3\ (critical)} \approx \sigma_c$ values. These near-critical effective confining stress levels will actually be reached first on the contacting (stress-transferring) 'asperities' which in the case of quite planar sheared surfaces, will tend to be significant 'islands' of contact. It is these which will compromise continued production, until re-fracking near-by, and repeating the cycle of fracturing-propping-shear stimulating-draining.

CONCLUSIONS

Hydraulic fractures generated at frequent intervals along horizontal well-bores, to produce unconventional shale gas, seem at present to be well separated from the nearer-surface water resources. A greater exploration and design challenge would arise if the present thousands of meters separation was reduced by potentially viable shallower gas resources.

Since microseismic activity significantly outside the hydraulic fracture-stimulated zones is registered, and since this activity is shear-induced, the production of shale gas depends more strongly than normally on a coupled-process of shear – dilation – permeability – stress – strength interaction, with non-linear rock mechanics input as an essential component. This is hardly seen so far in petroleum geomechanics papers and courses.

It is not sufficient to invoke linear Mohr-Coulomb geomechanics when both the fractures and matrix are to go through many tens of MPa stress change during even one year of first-stage production.

Non-linearity and the problem of reaching the brittle-ductile transition and perhaps critical-state may arise in the lower modulus lower strength shales, and it will arise first in the stress-transferring 'island-asperities'.

The 'island asperities' where initial leading-edge shearing may have been responsible for the microseismic signals, should be as small as possible to maximize drainage area. This ideal is probable in the Barnett shale, but in the weaker shales, fracture deformation and increased contact area during the first year of production will tend to compromise continued productivity, due to reducing fracture areas remaining for flow.

In a conventional fractured reservoir like Ekofisk, water drive is the answer to delaying the non-linear sheared-fracture closure. So far it has been necessary to minimize water and maximize proppant in gas-shales. *Quo-vadis* needs answers.

REFERENCES

Bandis, S., Lumsden, A.C. & Barton, N. (1983). Fundamentals of rock joint deformation. *Int. J. Rock Mech. Min. Sci. and Geomech. Abstr.* Vol. 20: 6: 249-268.

Barton, N. (1973). Review of a new shear strength criterion for rock joints, *Engineering Geology*, Elsevier, Amsterdam, Vol. 7, pp. 287-332.

Barton, N. (1976). The shear strength of rock and rock joints. I*nt. J. Rock Mech. Min. Sci. and Geomech. Abstr*., Vol. 13, No. 9: p. 255-279

Barton, N. (1981). Hydraulic fracturing to estimate minimum stress and rockmass stability at a pumped hydro project. Proc. of *Workshop on Hydraulic Fracturing Stress Measurements*, Monterey, USA.

Barton, N., Bandis, S. & Bakhtar, K. (1985). Strength, deformation and conductivity coupling of rock joints. *Int. J. Rock Mech. & Min. Sci. & Geomech. Abstr*. 22: 3: p.121-140.

Barton, N. (1986). Deformation phenomena in jointed rock. 8th Laurits Bjerrum Memorial Lecture, Oslo. *Geotechnique*, Vol. 36: 2: p.147-167.

Barton, N. (2006). *Rock Quality, Seismic Velocity, Attenuation and Anisotropy.* Taylor & Francis, UK & Netherlands, 729 p.

Barton, N. (2007). Thermal over-closure of joints and rock masses and implications for HLW repositories.

Proc. of *11th ISRM Congress*, Lisbon, Vol. 1, p. 109-116.

Barton, N. (2014). Non-linear behaviour for naturally fractured carbonates and frac-stimulated gas-shales. First Break, EAGE.

Dusseault, M. (2013). Geomechanical aspects of shale gas development. Keynote lecture, Eurock2013, Wroclow, Poland. *Rock Mechanics for Resources, Energy and Environment. Kwasniewski & Lydzba*. Taylor and Francis, London, p. 39-56.

Fisher, K. and N. Warpinski (2011). Hydraulic fracture-height growth: real data. *SPE Annual Technical Conference*, Denver, Colorado, USA. SPE 151597, 18p.

Ghassemi, A. and R. Suarez-Rivera (2012). Sustaining fracture area and conductivity of gas shale reservoirs for enhancing long-term productivity and recovery. RPSEA, (Research Partnership to Secure Energy for America). Final report, 08122-48, 253p.

Gutierrez, M., Oino, L., and Nygard, R. (2000). Stress-dependent permeability of a demineralised fracture in shale, *Marine and Petroleum Geology*, **17(8)**, p. 895-907.

Han, G. (2011). Natural fractures in unconventional reservoir rocks: identification, characterization, and its impact to engineering design. Proc. 45th US Rock Mechanics/Geomechanics Symp., San Fransisco, USA.

King, G. (2010). Thirty years of gas shale fracturing: what we have learned? SPE 133456. *The SPE Annual Technical Conference and Exhibition, p.19-22 September 2010*. Florence, Italy.

Makurat, A., Barton, N., Rad, N.S. & Bandis, S. (1990). Joint conductivity variation due to normal and shear deformation. *Int. Symp. on Rock Joints.* Loen 1990. Proc, p.535-540, Balkema.

McLennan, J. and D. Potocki (2013). Hydraulic fracturing complexity: Interaction between hydraulic and natural fractures. AAPG Workshop. *Geomechanics and Reservoir Characterization of Shales and Carbonates*. Baltimore, USA.

Olsson, R. & Barton, N. (2001). An improved model for hydro-mechanical coupling during shearing of rock joints. *Int. J. Rock Mech. Min. Sci. & Geomech. Abstracts*, 38: p. 317-329. Pergamon.

Singh, M., Raj, A. and B. Singh (2011). Modified Mohr-Coulomb criterion for non-linear triaxial and polyaxial strength of intact rocks. *Int. J. Rock Mech. Mining Sci.*, 48(4), p.546-555.

Warpinski, N. (2012). Measurements and observations of fracture height growth. EPA Workshop.

Warpinski, N., J.Du U. Zimmer. (2012). Measurements of hydraulic-fracture-induced seismicity in gas shales. SPE 151597. SPE Hydraulic Fracturing Technology Conference, Texas, USA.

Zoback, M., S. Kitasei and B. Copithorne. (2010). Addressing the environmental risks from shale gas development. Worldwatch Institute, *Natural Gas and Sustainable Energy Initiative*. Briefing P1, p. 1-18.